Role of the Arginine-45 Salt Bridge in Ligand Dissociation from Sperm Whale Carboxymyoglobin As Probed by Photoacoustic Calorimetry†

Judy A. Westrick and Kevin S. Peters*
Department of Chemistry and Biochemistry, University of Colorado, Boulder, Colorado 80309
J. Dezz Ropp and Stephen G. Sligar*
Departments of Biochemistry and Chemistry, University of Illinois, Urbana, Illinois 61801
Received November 7, 1989; Revised Manuscript Received February 8, 1990

ABSTRACT: The dynamics of the enthalpy and volume changes found in the photodissociation of CO from sperm whale carboxymyoglobin and two site-directed mutants in which arginine-45 is replaced by glycine and asparagine are examined by photoacoustic calorimetry. An intermediate is observed whose lifetime at 20 °C is 700 ns. The enthalpy of the intermediate increases by ~7 kcal/mol upon replacing arginine-45 with either asparagine or glycine. These observations support recent proposals that an arginine-45 salt bridge is broken upon ligand dissociation.

Establishing the relationship between the molecular motion of a protein and its function is essential for the development of models for enzyme action. Although X-ray structures of proteins provide a wealth of information for the understanding of protein function, the picture is incomplete without full characterization of intermediate states that intervene in protein action. Minimally, one would like to understand how the protein structure controls the dynamics and energetics of substrate binding and catalytic function. A great variety of experimental techniques have been developed that provide information relating to kinetics of protein function as well as structure of intermediate species; these techniques include time-resolved UV–vis absorption, Raman, EPR, NMR, and IR spectroscopy. Molecular dynamic computer simulations of proteins provide a detailed description of atomic motion on the subnanosecond time scale.

One source of information that has been notably lacking in the study of protein function is energetics of short-lived species, as experimental methods have not been available to measure reaction energies on the nanosecond and microsecond time scales. However, a new experimental method, time-resolved photoacoustic calorimetry, has recently been developed that is sensitive to the time dependence of the energetics of transient species as well as molecular motion in proteins (Peters & Snyder, 1988).

In a recent publication (Westrick et al., 1987) we presented the results of our initial study of the time-resolved photoacoustic calorimetry of sperm whale carboxymyoglobin in Tris buffer at pH 8.0. This study addressed the question of the pathway by which the ligand, carbon monoxide, diffuses from the heme pocket to the solvent and the corresponding energetics, dynamics, and volume changes associated with this process. We found that photodissociation of the carbon monoxide produced within 100 ns an intermediate state whose enthalpy difference with respect to carboxymyoglobin is thermoneutral and whose formation is accompanied by a negative volume change. The intermediate, in turn, decayed on the 700-ns time scale to form deoxymyoglobin.

The negative volume change and thermoneutral enthalpy change for the intermediate formation was surprising, as it was anticipated that the enthalpy of geminate pair formation would be in excess of the overall binding energy, 17 kcal/mol (Rudolph et al., 1972). It was speculated that the excess heat evolved during geminate pair formation may be the result of protein restructuring, such as the breaking of a salt bridge, or the release of a proton to the buffer. In this paper we will examine the role of the salt bridge between Arg-45 and the heme's propionate side chain by replacing the Arg-45 with either Gly or Asn through site-directed mutagenesis. In addition, the possibility of proton release or uptake is addressed by comparing the energetics in phosphate and Tris buffer at pH 8.0.

Experimental Procedures

Site-Directed Mutagenesis. The *Pst*I–*Kpn*I fragment of pMb413a [synthetic sperm whale myoglobin as described in Springer and Sligar (1987)] was subcloned into M13mp19 (New England Biolabs). All subsequent manipulations were performed according to the method of Taylor et al. (1985), utilizing the Amersham oligonucleotide-directed in vitro mutagenesis system. Mutations were selected by the loss of a *Pvu*I site. The mutation frequency was 75–85% on the basis of loss of the *Pvu*I site. Mutations were identified by DNA sequencing as described elsewhere (Sanger et al., 1977). The mutant genes were subcloned back into pUC19 for subsequent expression in *Escherichia coli* strain TB-1 (Bethesda Research Laboratories). For both R45G[1] and R45N, the mutant oligonucleotide was 3′-TTTAAGCTA$^{T}/_{C}{}^{T}/_{C}$AAAGTTTGTA-GA-5′ and was obtained from the Genetic Engineering Facility, University of Illinois, Urbana, IL.

Protein Purification. The mutant sperm whale myoglobin proteins R45G and R45N were purified as described elsewhere (Springer & Sligar, 1987).

Apparatus. The time-resolved photoacoustic calorimeter employs a PRA nitrogen-pumped dye laser (LN1000/LN102) operating at 1 Hz, 510 nm, pulse width 500 ps, and an energy of 17 μJ for excitation. The sample is held, under anaerobic conditions, in a 1 cm × 1 cm cuvette embedded in an alu-

† This research was supported by grants from the National Institutes of Health (GM36859, GM3375, and GM31756).

[1] Abbreviations: R45G, the site-directed mutant of sperm whale myoglobin that contains glycine at position 45 instead of the native arginine; R45N, the site-directed mutant of sperm whale myoglobin that contains asparagine at position 45 instead of the native arginine.

0006-2960/90/0429-6741$02.50/0

minum block thermostated by a Haake A80 temperature controller to ±0.1 °C. The acoustic waves are detected by a 0.5-MHz lead zirconate–lead titanate piezoelectric transducer whose output voltage is amplified (Panametric ultrasonic preamp) and recorded by a Gould 4072 digital oscilloscope, 100 MHz. The data are transferred to an IBM XT computer where each acoustic wave is normalized to the laser energy measured by a Laser Precision, Rj 7000, pyrolytic probe.

Sample Preparation. Sperm whale metmyoglobin (Sigma) is dissolved in 0.1 M phosphate buffer or Tris buffer and adjusted to pH 8.0. The solution is filtered through a 0.45-μm Millipore filter and then stands overnight. Deoxygenation is achieved by stirring under N_2 at 22 °C for 2 h. Deoxymyoglobin is produced by reduction with a 10-fold excess of sodium dithionate. Carboxymyoglobin is formed by stirring deoxymyoglobin under a CO atmosphere.

Thermal Expansion Coefficients. Our prior method of data analysis consisted of correlating the photoacoustic amplitudes with ratios of thermal expansion coefficients at two temperatures (Westrick et al., 1987). The ratio of thermal expansion coefficients was obtained from the ratio of the acoustic wave amplitudes of the calibration compound at two temperatures. This method tacitly assumes that the instrument response function does not vary with temperature. However, further experiments revealed that the coupling of the microphone to the cuvette is slightly dependent upon temperature. In the present method of data analysis the amplitudes of the photoacoustic waves are directly correlated with $\beta/C_p\rho$, where β is the thermal expansion coefficient for the solution, C_p the heat capacity, and ρ the density. All three of these quantities are temperature dependent. In order to obtain $\beta/C_p\rho$ for 0.1 M phosphate or 0.1 M Tris buffers at pH 8.0, the photoacoustic wave amplitudes of bromocresol purple in distilled water at dilute concentration, <1 μM, and deoxymyoglobin in the buffer solution are compared as a function of temperature. The ratio of the acoustic wave amplitudes for the two solutions directly reflects the ratio of $\beta/C_p\rho$ for the two solutions. Since the values for distilled water as a function of temperature are known, the values for the protein solution can be obtained.

Data Analysis

The acoustic signal, S, resulting from the photolysis of a protein such as carboxymyoglobin is the result of the expansion or contraction, ΔV, of the irradiated sample:

$$S = K\Delta V \tag{1}$$

where K is a constant of the instrument response. There are two contributions to the overall volume of expansion: a thermal component, ΔV_{th}, and a conformational change component, ΔV_{con}, due to a change in the volume of the protein or electrostriction of the solvent. The thermal component ΔV_{th} is caused by the deposition of thermal energy to the solvent, ΔE, as the excited state of the protein decays to produce reactive intermediates:

$$\Delta V_{th} = (\beta/C_p\rho)\Delta E \tag{2}$$

The term β represents the thermal expansion coefficient for the solvent, C_p the heat capacity of the solution, and ρ the density of the solution. The photoacoustic signal is expressed as

$$S = K(\Delta V_{th} + \Delta V_{con}) = K[(\beta/C_p\rho)\Delta E + \Delta V_{con}] \tag{3}$$

For the purpose of calibration, a compound is used whose photochemistry converts the photoenergy into heat only and undergoes no conformational changes on the time scale of the instrument response. The calibration compound used in these studies is deoxymyoglobin (Westrick et al., 1987). The photoacoustic signal from the calibration compound, S_{cal}, is

$$S_{cal} = K(\beta/C_p\rho)E_{h\nu} \tag{4}$$

where $E_{h\nu}$ is the energy of the photon expressed in kcal/mol. The ratio of the acoustic wave amplitudes for the sample of interest to the calibration compound is

$$\phi = S/S_{cal} = (\Delta E/E_{h\nu}) + (\Delta V_{con}/[(\beta/C_p\rho)E_{h\nu}]) \tag{5}$$

In this expression ϕ is dependent upon temperature as β, C_p, and ρ are temperature dependent. We define

$$F(T) = \beta/C_p\rho \tag{6}$$

which leads to, upon rearrangement

$$E_{h\nu}\,\phi = \Delta E + \Delta V_{con}/F(T) \tag{7}$$

It is assumed that ΔE and ΔV_{con} are independent of temperature. Correlating $\phi E_{h\nu}$ with $1/F(T)$ yields ΔE and ΔV_{con}. The overall enthalpy reaction, ΔH, is then determined by

$$\Delta H = E_{h\nu} - \Delta E \tag{8}$$

The experimentally observed photoacoustic signal, $E(t)$, results from the convolution of the instruments response function, $T(t)$, with a time-dependent source that generates acoustic waves, $H(t)$, which results from time-dependent enthalpy and volume changes within the system:

$$E(t) = H(t)T(t) \tag{9}$$

If there is only a single decay, with kinetics k, during the time scale of the experiment then $H(t)$ has the form

$$H(t) = \phi \exp(-t/\tau) \tag{10}$$

where $\tau = 1/k$. The parameter ϕ is defined in eq 5. For two sequential decays occurring on the time scale of the instrument response

$$A \xrightarrow{k_1} B \xrightarrow{k_2} C \tag{11}$$

$H(t)$ will have the form

$$H(t) = \phi_1 \exp(-t/\tau_1) + [\phi_2 k_1/(k_2 - k_1)][\exp(-t/\tau_1) - \exp(-t/\tau_2)] \tag{12}$$

The quantities ϕ_1 and ϕ_2 for each kinetic process are defined in eq 5. The values ϕ_1, ϕ_2, τ_1, and τ_2 are obtained by deconvolution of the acoustic waves. The deconvolution procedure involves calculating an $H(t)$ wave assuming a set of parameters, ϕ_k and τ_k. The $H(t)$ wave is then convoluted with the instrument response function, $T(t)$ obtained from the calibration compound to produce an $E_{calc}(t)$ wave. The $E_{calc}(t)$ wave is then compared to the experimental $E_{exp}(t)$ wave by evaluation of the sum of the residuals. The fitting parameters ϕ_k and τ_k are then varied to minimize the residuals (Westrick et al., 1987).

Results

The photoacoustic spectrum of 130 μM carboxymyoglobin (MbCO) in 0.1 M phosphate buffer, pH 8.0, at 20 °C is shown in Figure 1. The wavelength of irradiation is 510 nm with an excitation energy of 17 μJ. The reference compound used to generate the instrument response function, the T-wave, is deoxymyoglobin (Mb) employed under identical conditions. There is a pronounced shift in time of the carboxymyglobin acoustic wave relative to the deoxymyoglobin, indicating that chemistry occurs on the time scale of the instrument response, approximataely 100 ns–20 μs. The photoacoustic spectrum

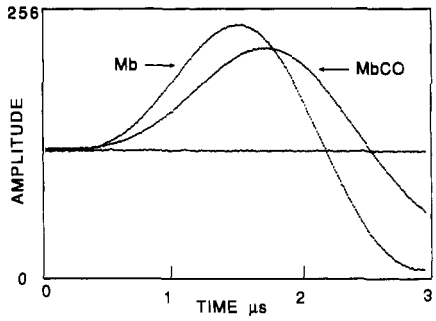

FIGURE 1: Photoacoustic spectrum of the calibration compound, 130 μM deoxymyoglobin (Mb), and the sample, 130 μM carboxymyoglobin (MbCO), at 20 °C, in 0.1 M phosphate buffer, pH 8.0, λ_{exc} = 510 nm.

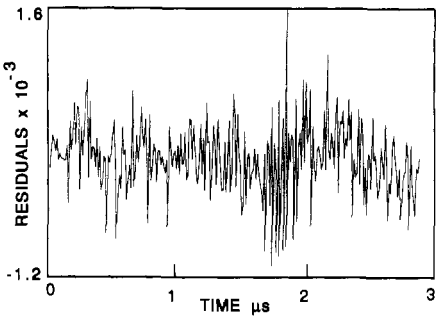

FIGURE 2: Residual spectrum from the difference between the experimental wave and the calculated wave for carboxymyoglobin at 15.1 °C assuming $H(t)$ has the form given by eq 12. The parameters are τ_1 = 1 ns, ϕ_1 = 0.073, τ_2 = 1144 ns, and ϕ_2 = 1.262. The maximum amplitude in the experimental acoustic wave of carboxymyoglobin is scaled to 1.0.

Table I: Enthalpy and Volume Changes Resulting from Photodissociation of CO from Carboxymyoglobin

	ΔH_1[a]	ΔH_{1+2}[a]	ΔV_1[b]	ΔV_{1+2}[b]
0.1 M phosphate	0.8 ± 1.4	9.9 ± 2.0	−9.0 ± 0.3	5.1 ± 0.5
0.1 M Tris	0.6 ± 2.2	11.3 ± 1.8	−9.2 ± 0.5	5.8 ± 0.4
R45N	8.7	12.3	−4.7	5.5
R45G	7.5	9.6	−3.8	7.8

[a] kcal/mol. [b] mL/mol.

of carboxymyoglobin in 0.1 M phosphate buffer, pH 8.0, was examined as a function of temperature, ranging from 29.4 to 11.7 °C. A total of eight separate experiments were carried out encompassing 53 data sets.

Since the photoacoustic wave for carboxymyoglobin is shifted in time with respect to the deoxymyoglobin wave, a transient species, whose lifetime is on the time scale of the instrument response, must exist. Assuming that only one transient decay is present, the observed acoustic waves were deconvoluted where $H(t)$ has the form expressed in eq 10. An acceptable fit could not be obtained (Rudzki et al., 1985). Next the deconvolution was carried out assuming that $H(t)$ has the form shown in eq 12; that is, two sequential decays are manifested in the carboxymyoglobin acoustic wave. In this procedure τ_1 was held constant at 1 ns while ϕ_1, ϕ_2, and τ_2 were varied. Holding τ_1 constant at 1 ns assumes that the first kinetic event is faster than the instrument response and cannot be temporally resolved; the instrument, however, is sensitive to its amplitude, ϕ_1. An example of the difference between the calculated wave, $E_{calc}(t)$, and the experimental wave, $E_{exp}(t)$, for MbCO at 15.1 °C is shown in Figure 2.

The values of ΔE and ΔV for each of the two decays are obtained through eq 7. Plots of $\phi_1 E_{h\nu}$ and $\phi_2 E_{h\nu}$ versus $C_p\rho/\beta$ are shown in Figure 3. The slope of a plot corresponds to ΔV_{con} for the reaction, and the intercept is ΔE for the reaction.

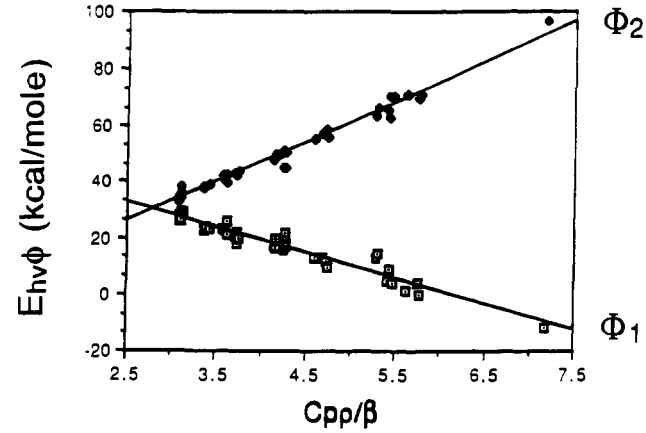

FIGURE 3: Plots of $\phi_1 E_{h\nu}$ vs $C_p\rho/\beta$ and $\phi_2 E_{h\nu}$ vs $C_p\rho/\beta$ for carboxymyoglobin in 0.1 M phosphate buffer at pH 8.0.

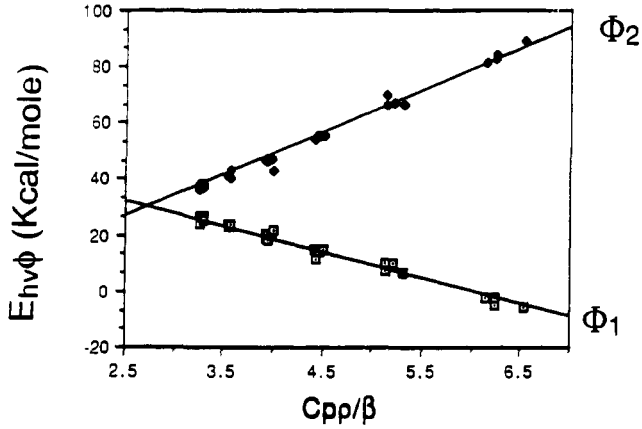

FIGURE 4: Plots of $\phi_1 E_{h\nu}$ vs $C_p\rho/\beta$ and $\phi_2 E_{h\nu}$ vs $C_p\rho/\beta$ for carboxymyoglobin in 0.1 M Tris buffer at pH 8.0.

Table II: Thermodynamic Activation Parameters from the Temperature Dependence of τ_2 for the Decay of the Geminate Pair

	ΔH^* (kcal/mol)	ΔS^* (cal K^{-1} mol^{-1})
0.1 M phosphate	10.4 ± 0.4	5.0 ± 1.6
0.1 M Tris	11.1 ± 0.3	7.6 ± 1.9
R45N	11.9	7.7
R45G	11.3	5.6

The enthalpy and volume changes for the intermediate state, ΔH_1 and ΔV_1, and the final state, ΔH_{1+2} and ΔV_{1+2}, are given in Table I.

A similar series of experiments were carried out for carboxymyoglobin in 0.1 M Tris buffer, pH 8.0. The temperature range was varied from 29.7 to 14.4 °C for 4 separate experiments with a total of 30 acoustic spectra. The results of these experiments, shown as plots of $\phi_1 E_{h\nu}$ and $\phi_2 E_{h\nu}$ versus $C_p\rho/\beta$, are illustrated in Figure 4. The resulting enthalpy and volume changes are given in Table I. It is noted that the values reported herein differ from those previously reported (Westrick et al., 1987). This difference is attributed to the temperature response of the microphone, which was not properly taken into account. The present method of data analysis circumvents this problem.

From the temperature dependence of τ_2, the enthalpy and entropy of activation for the second kinetic process can be obtained. Within the framework of activated complex theory, a thermodynamic formulation of the rate constant yields

$$\ln (k/\{k_b T/h\}) = \Delta S^*/R + (-\Delta H^*/RT) \quad (13)$$

so that a correlation of ln $(k/\{k_b T/h\})$ versus $1/RT$ yields a slope whose value is the enthalpy of activation, ΔH^*, and an

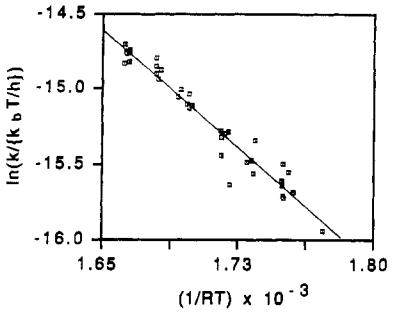

FIGURE 5: Plot of ln $(k/\{k_bT/h\})$ vs $1/RT$ for the second kinetic process, τ_2, for carboxymyoglobin in 0.1 M phosphate buffer at pH 8.0.

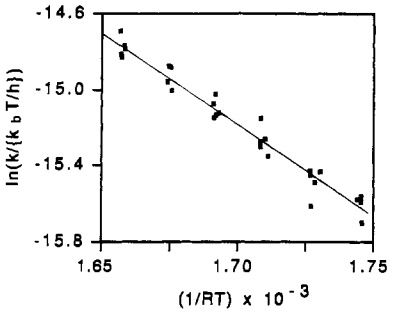

FIGURE 6: Plot of ln $(k/\{k_bT/h\})$ vs $1/RT$ for the second kinetic process, τ_2, for carboxymyoglobin in 0.1 M Tris buffer at pH 8.0.

intercept whose value is proportional to the entropy of activation, $\Delta S^{\ddagger}$. The plots for carboxymyoglobin in 0.1 M phosphate and 0.1 M Tris buffer are shown in Figures 5 and 6, and the resulting values for the enthalpy and entropy of activation are given in Table II.

The photoacoustic spectra of two mutants of sperm whale carboxymyoglobin were examined in 0.1 M phosphate buffer at pH 8.0. The mutants were formed by replacing Arg-45 with either Asn or Gly. Because of limited quantities of sample, only two separate experiments were run for each mutant and only two temperatures, 30 and 20 °C, were examined. In addition, the calibration compound used to generate the instrument response function, the T-wave, was wild-type sperm whale metmyoglobin. From previous studies we have found that metmyoglobin and deoxymyoglobin produce the same acoustic waves within the resolution of the experiment. An example of the photoacoustic wave for R45N at 20 °C in 0.1 M phosphate buffer, pH 8.0, is shown in Figure 7. The enthalpy and volume changes for the two mutants are given in Table I, and the entropy and enthalpy of activation for the second kinetic process are given in Table II. A reaction energy diagram for wild-type carboxymyoglobin and R45N is shown in Figure 8.

Discussion

In recent years there has been an extensive discussion as to the pathway by which the carbon monoxide ligand diffuses from the heme pocket to the solvent (Antonine et al., 1971; Case & Karplus, 1979; Czerminski & Elber, 1988; Kuriyan et al., 1986). Crystallographic studies of metmyoglobin reveal a salt bridge interaction between Arg-CD3 (Arg-45) and the propionate side chain of one of the heme's pyrroles (Perutz & Mathews, 1966; Takano, 1977a,b). Upon the binding of CO, there is a small displacement of the distal histidine, His-E7, which perturbs the salt bridge interaction, resulting in 50% of the population having salt bridges intact (Kuriyan et al., 1986). The binding of ethyl isocyanide causes His-E7 to exist in at least two positions, one of which points outward,

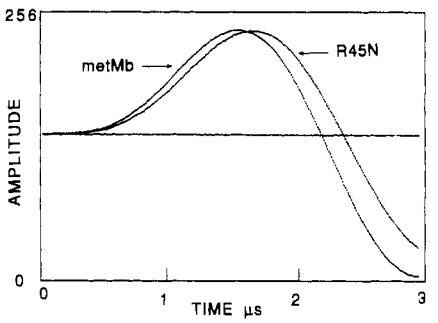

FIGURE 7: Photoacoustic spectrum of the calibration compound, metmyoglobin (OD_{510nm} = 0.40), and the sample, R45N (OD_{510nm} = 0.42), at 20 °C, in 0.1 M phosphate buffer, pH 8.0, and λ_{exc} = 510 nm.

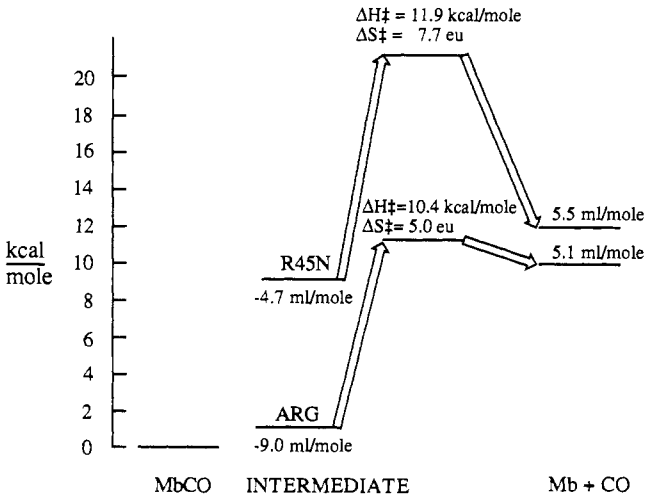

FIGURE 8: Enthalpy and volume changes for photolysis of carboxymyoglobin, wild type (Arg), and R45N in 0.1 M phosphate buffer at pH 8.0.

resulting in the disruption of the salt bridge (Johnson et al., 1989). The binding of large ligands such as an imidazole (Bolognesi et al., 1982) or a phenyl group (Ringe et al., 1984) forces His-E7 to point out of the heme pocket and Arg-CD3 to be displaced into the solvent, totally disrupting the salt bridge. This movement of His-E7 away from the heme pocket and disruption of the salt bridge serves to create a channel from the heme pocket to the solvent. It is through this channel that ligand diffusion is proposed to occur (Ringe et al., 1984; Johnson et al., 1989).

The role of the corresponding salt bridge in human myoglobin, which differs from sperm whale myoglobin in 25 positions in the primary sequence and for which no X-ray structure is available, has been addressed by mutating the lysine at position 45 to an arginine (Lambright et al., 1989). Boxer and co-workers note that although this is a conservative mutation that still allows for the formation of a salt bridge, they do observe minor changes in the on and off rates for CO binding, thus demonstrating that residue 45 is somehow involved in determining ligand access to the heme pocket (Lambright et al., 1989). It should be mentioned that the on and off rates of CO, O_2, and a series of isocyanide derivatives have been measured for the sperm whale myoglobin mutants described in this publication and will be reported elsewhere (T. Carver, J. Oslon, J. D. Roop, and S. C. Sligar, manuscript in preparation). It is important to note from these investigations, however, that although the CO on and off rates for the sperm whale myoglobin R45 mutants and the human myoglobin K45 mutants change by roughly the same factor, the exact role of the residue at position 45 as it pertains to

ligand access into the heme pocket is still uncertain.

Prior to our initial photoacoustic study, little was known about the energetics of intermediate states encountered in the dissociation of carbon monoxide from myoglobin at room temperature. Frauenfelder and co-workers (Austin et al., 1975) have studied the temperature dependence of the kinetics for the association and dissociation of carbon monoxide from sperm whale myoglobin in a glycerol–water mixture. To account for the kinetic behavior of transient species for temperatures ranging from 40 to 350 K, three intermediates were proposed to intervene between the carboxymyoglobin and fully dissociated deoxymyoglobin. The enthalpy difference between carboxymyoglobin and the first intermediate species, presumably the geminate pair where the CO is thought to be in the heme pocket, is approximately 18 kcal/mol.

The kinetics for the dissociation and association of carbon monoxide in myoglobin at room temperature have been investigated by flash photolysis. The photochemical dissociation of CO from the iron to form the geminate pair occurs within 350 fs (Martin et al., 1983). The geminate pair then decays on the time scale of 180 ns at 22 °C, with 4% recombining to form carboxymyoglobin and 96% dissociating to deoxymyoglobin and free carbon monoxide (Henry et al., 1983).

Given the previous studies on the kinetics and energetics of the geminate pair, it is surprising to find the photoacoustic data revealing an intermediate whose lifetime at 20 °C is 700 ns and whose enthalpy change is 1 kcal/mol and volume change is (−) 9.0 mL/mol relative to carboxymyoglobin. The kinetics of the 700-ns intermediate are clearly different from the 180-ns decay kinetics of the geminate pair observed in flash photolysis, suggesting that the intermediate is a species distinct from the geminate pair. Furthermore, the 18 kcal/mol enthalpy change for the formation of the geminate pair, obtained from low-temperature kinetic studies (Austin et al., 1975), differs from the 1 kcal/mol enthalpy change for formation of the intermediate. To account for this difference, it is postulated that the breaking of a Arg-45 salt bridge may contribute to the additional heat release observed at room temperature, for in a low-temperature matrix it may not be possible for the salt bridge to break due to the inability of the low-temperature glycerol–water matrix to reorganize to accommodate the charges. Another possible contribution to the 18 kcal/mol difference is that at room temperature the heat of protonation of the buffer may be manifested in the enthalpy change for intermediate formation (Ort & Parson, 1979). In a low-temperature glycerol–water matrix, proton release from the protein may not occur.

In order to ascertain whether the heat of protonation of the buffer is contributing to the enthalpy change for the formation of the intermediate, the photoacoustic spectrum for sperm whale myoglobin was examined in both Tris and phosphate buffers at pH 8.0. If during the formation of the intermediate one or more amino acids undergo a shift in pK_a as a result of structural changes within the protein, then a proton could be released to the solvent and bind to the buffer with subsequent heat release. If a proton is released, then the energetics will be dependent upon the identity of the buffer (Ort & Parson, 1979). For the buffer Tris, protonation leads to a heat release of 11 kcal/mol, while the heat released upon the protonation of phosphate is only 1 kcal/mol (Ort & Parson, 1979). However, from Table I, when the photoacoustic spectrum was examined in Tris and phosphate buffers, within experimental error, the energetics of the intermediate state as well as the final state are independent of the buffer, suggesting that there is no net change relative to carboxymyoglobin in the state of protonation of the intermediate or deoxymyoglobin.

If the breaking of the Arg-45–propionate salt bridge is involved in the ligand dissociation process and occurs upon the formation of the intermediate, then the enthalpic and volume changes associated with the rupture of the salt bridge will be manifested in the overall energetics and volume changes. Regrettably, little is known regarding the values of the enthalpy and volume changes for the breaking of salt bridges in proteins (Kauzmann, 1959). It is anticipated that when a salt bridge breaks, heat will be released due to increased solvation of charges, and this will be accompanied by a decrease in volume for the system due to the electrostriction of the solvent by the charges (Rodgers et al., 1988; Heremans, 1982).

When Arg-45 is replaced by either Asn or Gly, the energetics and volume changes for intermediate formation are perturbed; the enthalpy increases by 7 kcal/mol and the magnitude of the negative volume change decreases by 5 mL/mol. The overall energetics, ΔH_{1+2}, and volume change, ΔV_{1+2}, do not change as a result of the amino acid substitution. These observations strongly suggest that, within the 100-ns resolution of the instrument, the salt bridge is broken in an intermediate state, which is a 7 kcal/mol exothermic process. The second decay process in native myoglobin is endothermic by approximately 10 kcal/mol. Of these 10 kcal/mol, 7 kcal/mol can be attributed to the reformation of the salt bridge on the basis of the mutant studies. The other 3 kcal/mol reflects some other enthalpic process. It is important to note that these studies reveal that intermediate formation involves the breaking of the Arg-45 salt bridge; they do not reveal, however, the pathway by which the ligand diffuses between the heme pocket and the solvent.

When the kinetics of the second decay process, τ_2, are examined over temperatures ranging from 11.7 to 29.4 °C, the decay times vary from 425 ns to 1.2 μs. Importantly, the kinetics are independent of the two buffer systems that were examined. Furthermore replacement of Arg-45 with Asn or Gly has no effect upon the kinetics, and hence the activation parameters, within the error of the experiment; see Table II. These findings suggest that the observed enthalpy of activation, $\Delta H^* = 11$ kcal/mol, and entropy of activation, $\Delta S^* = 7$ cal K^{-1} mol^{-1}, do not involve the re-formation of the salt bridge in the transition state; it is only after the rate-determining step that the salt bridge reforms by an endothermic process.

The kinetics of the second decay process, as measured by photoacoustic calorimetry, are very different from those measured for the decay of the geminate pair by nanosecond flash photolysis (Henry et al., 1983). The value of τ_2 at 20 °C is 700 ns and the decay dynamics of the geminate pair at 22 °C is 180 ns. Clearly, the two experiments are measuring two different processes. In flash photolysis the time dependence of the difference spectrum between carboxymyoglobin and deoxymyoglobin absorption spectra is monitored and is presumably sensitive to the diffusion time of the CO out of the heme pocket; it is not directly sensitive to the diffusion of the CO out of the protein matrix and into the solvent. If the diffusion of the CO out of the heme pocket and into the protein matrix involves only a small change in enthalpy and volume, photoacoustic calorimetry would not be sensitive to this process and the 180-ns transient would not be observed.

There is then the question of the nature of the process that involves an enthalpy and entropy of activation of 11 kcal/mol and 7 cal K^{-1} mol^{-1}, respectively, and is endothermic by ~3 kcal/mol, where the remaining 7 kcal/mol of the endothermic process is attributed to salt bridge formation. One possibility

is that the diffusion of CO out of the protein matrix and into the solvent is being monitored. From X-ray crystallographic analysis of the structure of myoglobins, there are no channels accessible for CO to diffuse directly into the solvent (Perutz & Mathews, 1966). Instead the protein must undergo structural reorganization to create a reduced barrier for ligand diffusion. Molecular dynamics simulations of ligand diffusion from the protein matrix into the solvent reveal that the entropy of activation for this process is negative and can be as large as -20 cal K^{-1} mol^{-1} (Case & Karplus, 1979; Kottalam & Case, 1988). However, the entropy of activation for the second kinetic process is positive.

An alternative process may involve the rapid diffusion of CO out of the protein matrix, which is then followed by a rate-limiting structural relaxation of the protein on the 700-ns time scale. Upon dissociation of the bound ligand from the ion, the protein undergoes a structural reorganization, one component of which is the breaking of the Arg-45 salt bridge. In addition, it is likely that there is a change in the packing of α-helices leading to an increase in solvation, causing the water molecules to become more highly ordered about the protein. Once the CO escapes the protein matrix, the protein structure will relax to the deoxy form. This relaxation will be accompanied by the release of water, causing a decrease in enthalpy and an increase in the entropy of the system (Privalov & Gill, 1988), and should have a positive entropy of activation. Once this rate-limiting structural reorganization has occurred, the salt bridge re-forms, accompanied by the further uptake of heat.

In summary, these photoacoustic calorimetry studies have revealed that upon CO dissociation from the iron the Arg-45–propionate salt bridge ruptures in the intermediate state. Following diffusion of CO out of the protein matrix, the protein apparently undergoes a structural relaxation on the 700-ns time scale, which is then followed by the re-formation of the salt bridge. The pathway by which CO diffuses out of the protein has yet to be experimentally identified. This will be the subject for further photoacoustic calorimetric studies.

References

Antonine, E., & Brunori, M. (1971) *Hemoglobin and Myoglobin in Their Reactions with Ligands*, North-Holland, Amsterdam, The Netherlands.

Austin, R. H., Beeson, K. W., Eisenstein, L., Frauenfelder, J., & Gunsalus, I. C. (1975) *Biochemistry 14*, 5355–5373.

Bolognesi, M., Cannillo, E., Ascenzi, P., Giacometti, G. M., Merli, A., & Brunori, M. (1982) *J. Mol. Biol. 158*, 305–315.

Case, D. A., & Karplus, M. (1979) *J. Mol. Biol. 132*, 343–368.

Czerminski, R., & Elber, R. (1988) Symposium on Oxygen Binding Heme Proteins: Structures, Dynamics, Function and Genetics, Pacific Grove, CA (Abstract PVII-4).

Henry, E. R., Sommer, J. H., Hofrichter, J., & Eaton, W. (1983) *J. Mol. Biol. 166*, 443–451.

Heremans, K. (1982) *Annu. Rev. Biophys. Bioeng. 11*, 1–21.

Johnson, K. A., Olson, J. S., & Phillips, G. N. (1989) *J. Mol. Biol. 207*, 459–463.

Kauzmann, W. (1959) *Adv. Protein Chem. 14*, 1–63.

Kottalam, J., & Case, D. A. (1988) *J. Am. Chem. Soc. 110*, 7690–7697.

Kuriyan, J., Wilz, S., Karplus, M., & Petsko, G. A. (1986) *J. Mol. Biol. 192*, 133–154.

Lambright, D. G., Balasubramanian, S., & Boxer, S. G. (1989) *J. Mol. Biol. 207*, 289–299.

Martin, J. L., Migus, A., Poyart, C., Lecarpentier, Y., Astier, R., & Antonette, A. (1983) *Proc. Natl. Acad. Sci. U.S.A. 80*, 173–177.

Ort, D. R., & Parson, W. W. (1979) *Biophys. J. 25*, 355–364.

Perutz, M. F., & Matthews, F. S. (1966) *J. Mol. Biol. 21*, 199–202.

Peters, K. S., & Snyder, G. J. (1988) *Science 241*, 1053–1057.

Privalov, P. L., & Gill, S. J. (1988) *Adv. Protein Chem. 39*, 191–234.

Ringe, D., Petsko, G. A., Kerr, D. E., & Ortiz de Montellano, P. R. (1984) *Biochemistry 23*, 2–4.

Rodgers, K. K., Pochapsky, T. C., & Sligar, S. G. (1988) *Science 240*, 1657–1659.

Rudolph, S. A., Boyle, S. O., Dresden, D. F., & Gill, S. J. (1972) *Biochemistry 11*, 1098–1101.

Rudzki, J. E., Goodman, J. L., & Peters, K. S. (1985) *J. Am. Chem. Soc. 107*, 7849–7854.

Sanger, F., Nicklen, S., & Coulson, A. R. (1977) *Proc. Natl. Acad. Sci. U.S.A. 74*, 5463–5467.

Springer, B. A., & Sligar, S. G. (1987) *Proc. Natl. Acad. Sci. U.S.A. 84*, 8961–8965.

Takano, T. (1977a) *J. Mol. Biol. 110*, 537–568.

Takano, T. (1977b) *J. Mol. Biol. 110*, 569–584.

Taylor, J. W., Ott, J., & Eckstein, F. (1985) *Nucleic Acids Res. 13*, 8764–8785.

Westrick, J. A., Goodman, J. L., & Peters, K. S. (1987) *Biochemistry 26*, 8313–8318.